# Polydopamine-Based Simple and Versatile Surface Modification of Polymeric Nano Drug Carriers

**Joonyoung Park,[†] Tarsis F. Brust,[‡] Hong Jae Lee,[§] Sang Cheon Lee,[§] Val J. Watts,[‡] and Yoon Yeo[†,⊥,∥,*]**

[†]Department of Industrial and Physical Pharmacy, Purdue University, 575 Stadium Mall Drive, West Lafayette, Indiana 47907, United States,
[‡]Department of Medicinal Chemistry and Molecular Pharmacology, Purdue University, 575 Stadium Mall Drive, West Lafayette, Indiana 47907, United States,
[§]Department of Maxillofacial Biomedical Engineering & Institute of Oral Biology, School of Dentistry, Kyung Hee University, Seoul 130-701, Korea,
[⊥]Weldon School of Biomedical Engineering, Purdue University, 206 South Martin Jischke Drive, West Lafayette, Indiana 47907, United States, and
[∥]Biomedical Research Institute, Korea Institute of Science and Technology, Hwarangno 14-gil 5, Seongbuk-gu, Seoul 136-791, Korea

**ABSTRACT** The surface of a polymeric nanoparticle (NP) is often functionalized with cell-interactive ligands and/or additional polymeric layers to control NP interaction with cells and proteins. However, such modification is not always straightforward when the surface is not chemically reactive. For this reason, most NP functionalization processes employ reactive linkers or coupling agents or involve prefunctionalization of the polymer, which are complicated and inefficient. Moreover, prefunctionalized polymers can lose the ability to encapsulate and retain a drug if the added ligands change the chemical properties of the polymer. To overcome this challenge, we use dopamine polymerization as a way of functionalizing NP surfaces. This method includes brief incubation of the preformed NPs in a weak alkaline solution of dopamine, followed by secondary incubation with desired ligands. Using this method, we have functionalized poly(lactic-*co*-glycolic acid) (PLGA) NPs with three representative surface modifiers: a small molecule (folate), a peptide (Arg-Gly-Asp), and a polymer [poly(carboxybetaine methacrylate)]. We confirmed that the modified NPs showed the expected cellular interactions with no cytotoxicity or residual bioactivity of dopamine. The dopamine polymerization method is a simple and versatile surface modification method, applicable to a variety of NP drug carriers irrespective of their chemical reactivity and the types of ligands.

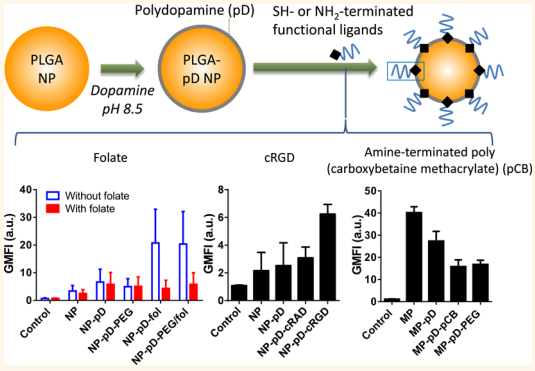


**KEYWORDS:** polymeric nanoparticles · drug delivery · surface modification · dopamine polymerization · cell–nanoparticle interactions

Polymeric nanoparticles (NPs) have been pursued as a promising carrier of anticancer drugs, which may improve drug distribution in tumors and reduce side effects on normal organs. To maximize drug delivery to tumors, NPs need to fulfill at least two requirements: to circulate with a long half-life until they reach target tumors (*stealth*) and to bind and enter the tumor cells (*target interaction*). The stealth effect is usually achieved by decorating the NP surface with hydrophilic, electrically neutral polymers such as polyethylene glycol (PEG), although it often interferes with effective interaction with tumor cells.[1,2] The NP–target interaction can be enhanced by attaching cell-specific ligands on NPs, which promote cell binding and uptake of NPs *via* specialized endocytosis mechanisms. Therefore, NPs are typically decorated with a stealth coating and cell-interactive ligands to achieve both effects, either simultaneously[3] or on demand.[4–6]

On the other hand, surface modification of polymeric NPs can be quite cumbersome unless the particle surface is chemically reactive. The lack of reactive functional groups necessitates activation of the NP surface with reactive linkers[7,8] or coupling agents,[9–12] followed by exhaustive purification processes to remove catalysts and excess reactants. Alternatively, NPs may be produced using prefunctionalized polymers, where functional ligands are covalently conjugated to polymers.[3,13–17] However, the synthesis of a polymer–ligand conjugate can be lengthy and inefficient and needs to be tailored for each ligand. Moreover, the ligand can alter the chemical properties of

* Address correspondence to yyeo@purdue.edu.

Received for review November 8, 2013 and accepted March 15, 2014.

**Published online March 15, 2014**
**10.1021/nn405809c**

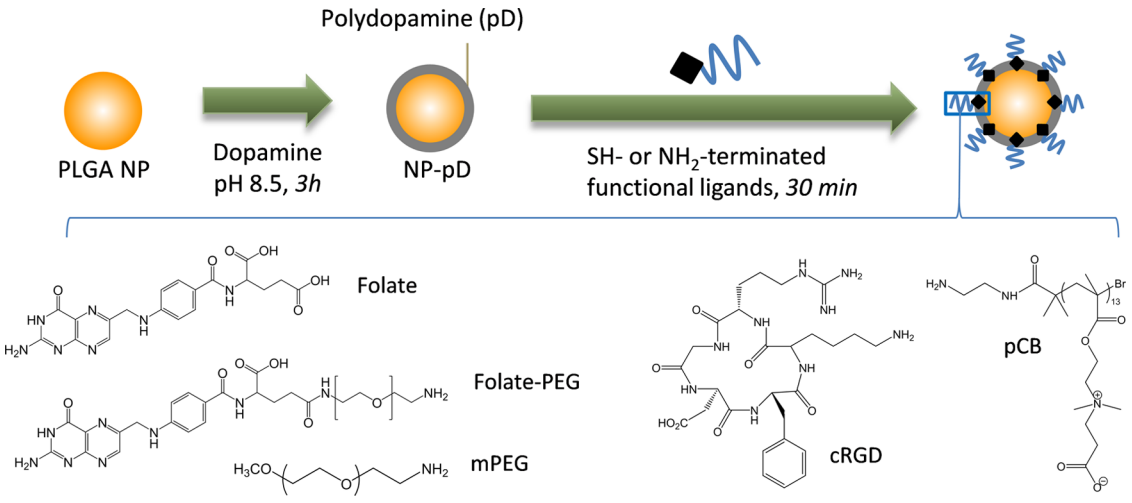


**Figure 1. Schematic diagram of surface modification of polymeric nanoparticles using dopamine polymerization.**

the conjugate (*e.g.*, increased hydrophilicity), compromising the ability of the polymer to encapsulate and/or retain a drug.

To overcome these challenges, we employ a simple and versatile surface modification method based on dopamine polymerization. In a weak alkaline condition (~pH 8−8.5) dopamine catechol is oxidized to quinone, which reacts with other catechols and/or quinones to form polymerized dopamine (pD).[18,19] As pD deposits on solid surfaces, it binds with functional ligands *via* Michael addition and/or Schiff base reactions to incorporate them into the surface layer.[18,19] The only requirement in this process is that the ligand molecules possess nucleophilic functional groups such as amine and thiol. Due to the simplicity and versatility, this principle has widely been exploited in functionalizing various types of substrates since its discovery in 2007.[18] For example, trypsin was immobilized on cellulose paper,[19] bivalirudin peptide on stainless steel,[20] polylysine on neuronal interface materials (gold, glass, platinum, indium tin oxide, liquid crystal polymer),[21] heparin[22] or albumin[23] on polyethylene membrane, lipase on magnetic NPs,[24] and avidin on yeast cells.[25] While the dopamine polymerization method has not been used in the modification of polymeric nano drug carriers, we hypothesize that the dopamine polymerization method can be applied to modify the surface of polymeric NPs, eliminating the complexity and inefficiency involved in traditional NP functionalization processes.

In this study, we demonstrate that poly(lactic-*co*-glycolic acid) (PLGA) NPs can be functionalized with various types of ligands *via* the dopamine polymerization method with unprecedented ease. Despite their popularity as a drug carrier, PLGA NPs do not readily interact with cells[26] and thus require surface modification to attain the ability. Our previous studies find that their functionalization is however challenged due to the lack of surface reactivity and technical complexity in the synthesis of new polymer derivatives.[14,27,28] Therefore, PLGA NPs are an ideal candidate for testing the new surface modification method. The dopamine polymerization method involves sequential incubation of PLGA NPs with dopamine and amine-terminated ligands in aqueous solution (Figure 1). We determined the optimal reaction conditions for functionalizing NPs, modified the NP surface with various ligands representing small molecules (folate), peptides (Arg-Gly-Asp, RGD), and polymers [poly(carboxybetaine methacrylate), pCB], and observed their interactions with target cells to confirm the effectiveness of this method. To estimate the safety of pD coating as a NP development tool, we also measured cytotoxicity and residual dopaminergic activity of the functionalized NPs.

## RESULTS AND DISCUSSION

**Prime-Coating with pD.** Prior to functionalization with ligands, NPs were incubated with dopamine under an oxidative condition (pH 8.5) to induce dopamine polymerization. Polymerized dopamine is known to bind tightly on solid surfaces *via* covalent and noncovalent interactions, forming a durable layer that serves as an intermediate for ligand incorporation.[29] In an earlier study using polymer films, Jiang *et al.* envisioned that oligomeric dopamine would first form nanoaggregates, which assemble into random aggregates on the micrometer scale and then deposit on the polymer surface.[30] Alternatively, Bernsmann *et al.* proposed that small oligomeric dopamines and monomers interact with the surface and then form interconnected layers on the surface.[31,32]

To determine how pD deposited on polymeric NP surfaces, we first incubated a fixed amount (0.5 mg) of polystyrene (PS) or PLGA NPs in an alkaline dopamine solution, varying the concentration from 0.25 to 1 mg/mL. Particle size was varied from 50 to 1000 nm in diameter to provide different surface areas for pD deposition. After 3 h incubation at room temperature, all NP

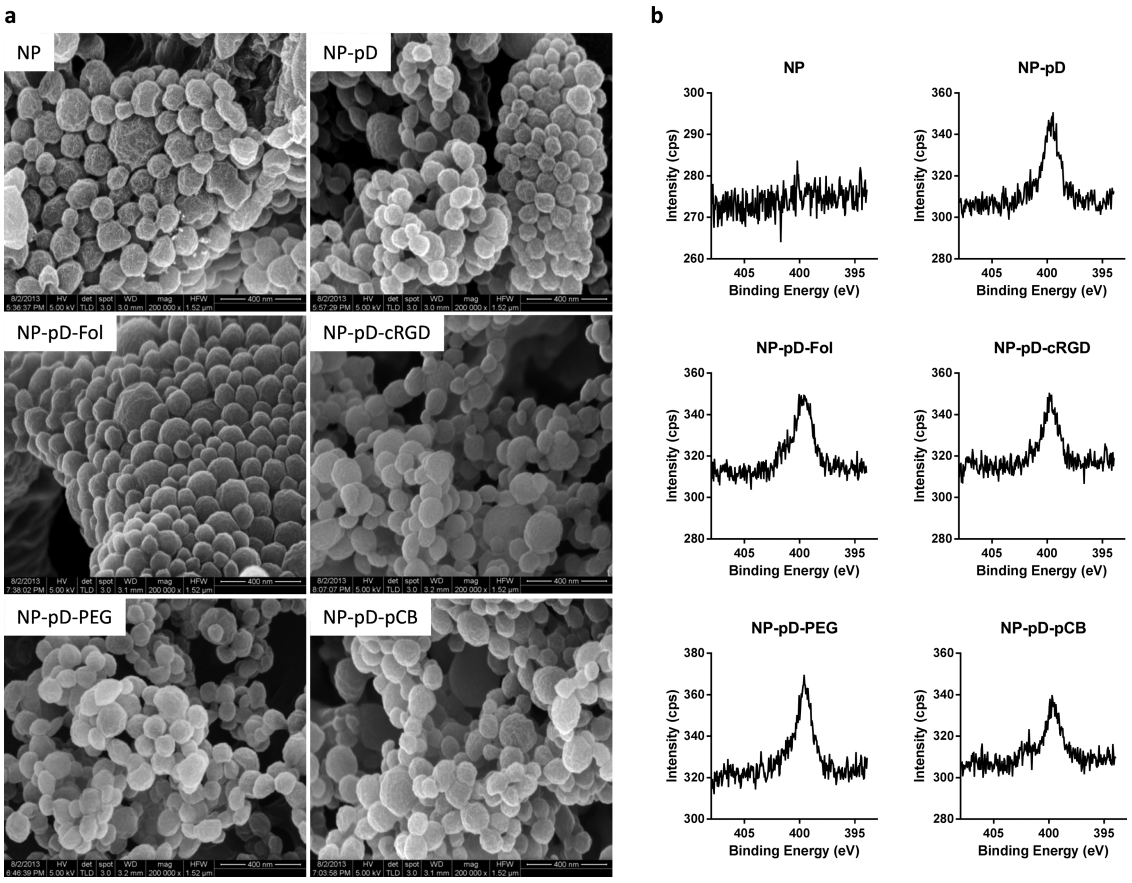


**Figure 2. (a) Scanning electron micrographs and (b) XPS N 1s spectra of PLGA NPs (NP), polydopamine prime-coated NPs (NP-pD), NPs coated with folate (NP-pD-Fol), cRGD (NP-pD-cRGD), mPEG (NP-pD-PEG), and pCB (NP-pD-pCB) *via* polydopamine.**

suspensions turned dark, indicating dopamine polymerization (Supporting Figure 1a), but we did not observe macroscopic black particles. We noticed that NP size increased at relatively high dopamine concentrations (0.75 and 1 mg/mL), especially when the NPs were relatively small (50 and 170 nm) (Supporting Figure 2). This result may be interpreted as increasing interparticulate interactions *via* surface-deposited pD, greater for small NPs with relatively large surface area per weight. Alternatively, the particle size increase with the increasing dopamine concentration may be interpreted as an indication of micrometric pD aggregates. To observe the configuration of pD deposition on NP surface, the PLGA NPs prime-coated in 0.5 mg/mL dopamine (NP-pD) were imaged with scanning electron microscopy (SEM). The freeze-dried NPs had a gray tint, clearly distinguished from the uncoated white NPs (Supporting Figure 1b). However, there was no noticeable difference between bare PLGA NPs (NP) and NP-pD under SEM (Figure 2a), nor was there a visible surface feature attributable to pD aggregates. Moreover, low-magnification SEM images (Supporting Figure 1c) showed that the collected NPs were homogeneous, free of extraneous particles in size and shape, indicating the absence of extra pD aggregates. Given the lack of macroscopic or microscopic pD aggregates, we speculate that pD deposits on NP surfaces as a thin film rather than particulate aggregates.

Bernsmann *et al.* reported that a 2 mg/mL dopamine solution formed only ~2 nm thick film on a silicon slide in 3 h.[31] In another study, a 2 mg/mL dopamine solution formed a 5−10 nm thick smooth film on the surface of a peptide nanowire after 16 h.[32] The pD coating formed on PLGA NPs with a 0.5 mg/mL dopamine solution in 3 h would likely be thinner than 2 nm, difficult to visualize by SEM. The difference of our observation from Jiang's model[30] may be attributable to several reasons, such as a lower concentration of dopamine solution (0.5 *vs* 2 mg/mL), a shorter incubation time (3 *vs* 24 h), the presence of substrate with a large surface area (NPs *vs* polymer film) during dopamine polymerization, and the hydrophilicity of the NP surface due to residual polyvinyl alcohol (PVA), which would reduce initial interfacial tension with dopamine solution. Taken together, our observations indicate that pD could be deposited on NP surfaces as a thin film, at least in the tested conditions, without forming pD aggregate impurities. Since NP size remained stable with dopamine concentration at 0.5 mg/mL or lower, all particles used in the rest of the study were prime-coated in 0.5 mg/mL dopamine solution.

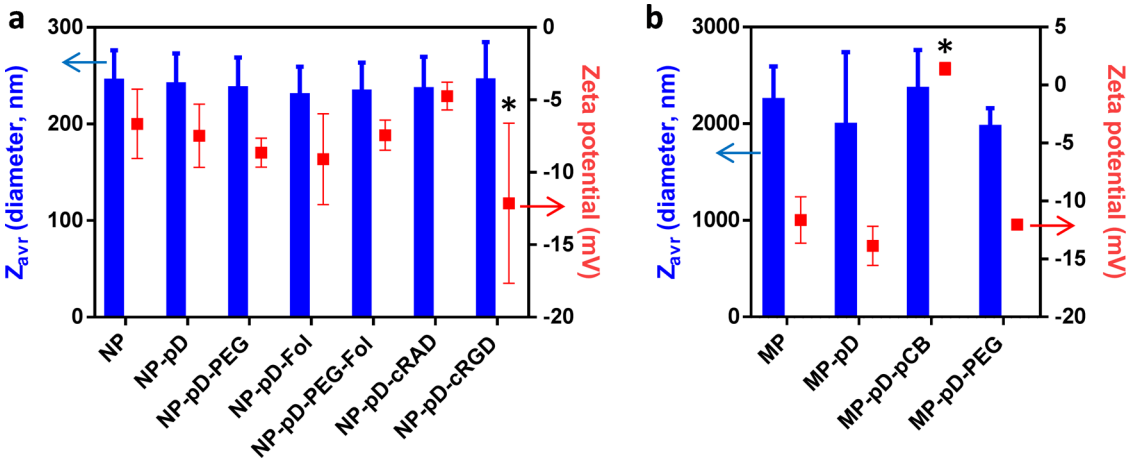


**Figure 3. Particle sizes and zeta potentials of NPs and MPs modified with different functional ligands *via* polydopamine. Data are expressed as averages and standard deviations of 3−8 batches of independently and identically prepared samples. Some data points have smaller standard deviations than the symbol size. *$p < 0.05$ *vs* NP or MP by two-tailed *t* test.**

**Functionalization of NP-pD.** After prime-coating of PLGA NPs with pD, amine-terminated functional ligands such as folate, cRGD, and a betaine polymer (pCB), representing small molecule, peptide, and polymer ligands, respectively, were incorporated with the NPs *via* the pD surface. Folate and cRGD are frequently used as ligands to target cancer cells overexpressing folate receptors[33] and neovasculature of tumors,[34] respectively. Amine-terminated betaine polymer (pCB) was synthesized as a new stealth coating with a potent antifouling effect.[35−38] All of the compounds had at least one primary amine per molecule, which reacts with pD *via* Schiff base reaction under an oxidizing condition.[39,40]

All the functionalized NPs showed (but bare NPs did not) a peak at ~399.6 eV in X-ray photoelectron spectroscopy (XPS) spectra, which corresponded to nitrogen (N 1s), verifying the presence of a pD layer (Figure 2b). A noticeable deviation was the shift of the deprotonated nitrogen peak shown with NP-pD-pCB, from 401.6 eV to 402.1 eV (Supporting Figure 3), indicative of quaternary nitrogen in the pCB polymer. There was no additional difference in XPS spectra among the functionalized NPs otherwise, likely due to the small quantity of conjugated ligands. Ligand incorporation did not significantly alter surface charge (Figure 3). NP, NP-pD, and the functionalized particles assumed negative charges at pH 7.4, reflecting the presence of carboxylate on the surface of the core PLGA NPs, evident from the XPS peak at 289.0 eV (Supporting Figure 4). The influence of pD coating and incorporated ligands on the surface charge is thought to be minimal, given the little difference in XPS between NP and the rest. However, we do not exclude a possibility that the negative charges partly reflect the deprotonated catechol hydroxyl groups of the surface pD. The only exception was the microparticles (MPs) modified with pCB (MP-pD-pCB), which showed no charge, probably due to pCB-induced hydration of the NP surface.[41] It is curious that the same effect was not seen in NP-pD-PEG or NP-pD-PEG-Fol with surface PEG. This may be attributable to the differences between pCB and PEG in the MW (pCB: 9.4 kDa, PEG: 5 kDa) and the hydration efficiency.[42] Ligand incorporation did not induce particle size increase (Figure 3). The particle size of NPs estimated from SEM (Figure 2a) was approximately 100 nm irrespective of the particle type, about half of the hydrodynamic diameters measured by dynamic light scattering (220−250 nm, Figure 3). This observation is consistent with our previous study[28,43] and attributable to NP aggregation in suspension. SEM did not reveal any visible difference in morphology among the functionalized NPs (Figure 2a).

To determine the relationship between the ligand feed and its incorporation in NPs, fluoresceinamine (FLA), a fluorescent dye with a primary amine, was incubated in varying concentrations (1−10 $\mu$g/mL) with a fixed amount of prime-coated NPs (NP-pD, 0.5 mg/mL). FLA was used in lieu of functional ligands to facilitate detection of the incorporated ligands. However, it was difficult to directly quantify the FLA incorporated in NPs due to the fluorescence enhancement by the pD layer (data not shown). Therefore, the incorporated FLA in NPs was indirectly quantified by subtracting the unincorporated dye from the feed. The amount of FLA incorporated in 0.5 mg/mL NP-pD reached a plateau of ~2.5 $\mu$g/mL (7.2 $\mu$M) (Supporting Figure 5), which translates to conjugation of $3.6 \times 10^4$ FLA molecules per NP with an average diameter of 200 nm (0.3 FLA/nm$^2$). Of note, all the functionalized NPs were created with 100−2000 $\mu$M of ligands for 0.5 mg/mL of NP-pD, sufficient excess of the maximum incorporated ligands.

**Toxicity and Biological Activity of pD Coating.** pD coating was shown to be nontoxic in various cell models and

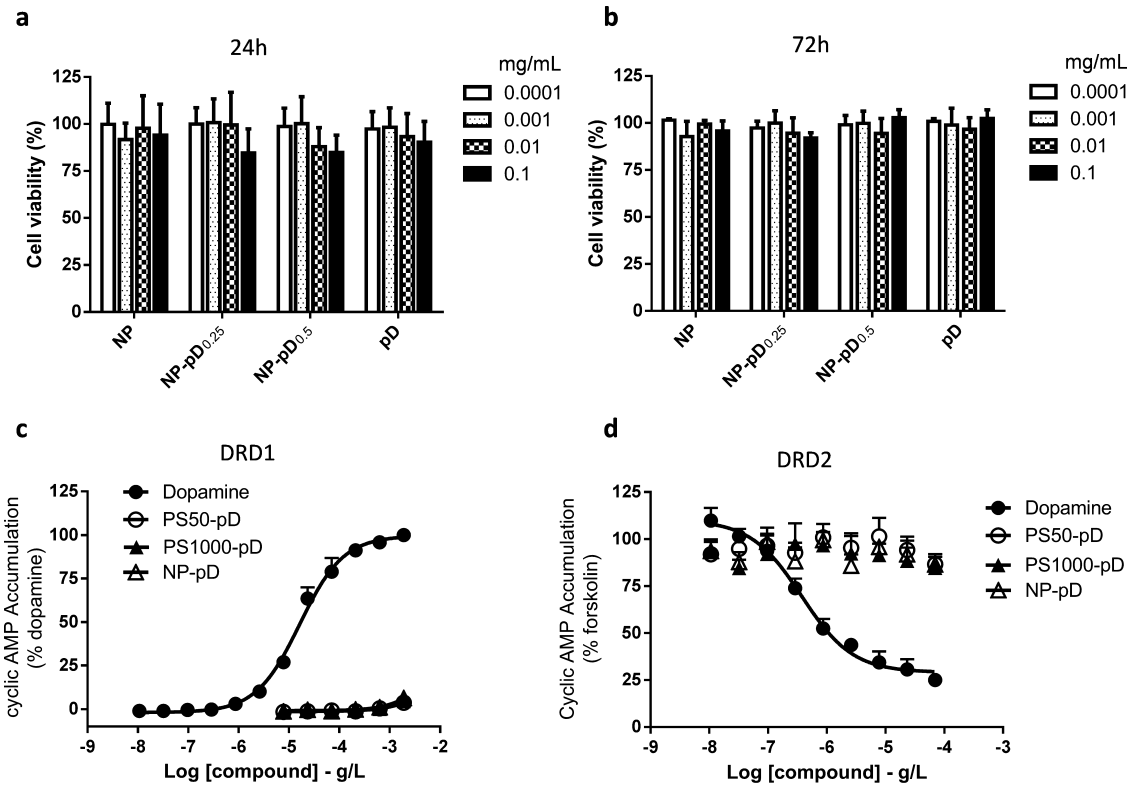


**Figure 4. (a, b) Cytotoxicity of NP, NP-pD, and polydopamine (pD) aggregates in NIH/3T3 fibroblast cells measured by the MTT assay. NP-pDs were prepared in 0.25 (NP-$pD_{0.25}$) or 0.5 mg/mL (NP-$pD_{0.5}$) dopamine solution, and pD aggregates were prepared by incubating dopamine hydrochloride solution in Tris buffer (10 mM, pH 8.5) for 3 h at room temperature with no NPs. NPs were added in the concentrations (mg/mL) indicated in the legends to the cells and incubated for (a) 24 h or (b) 72 h. Data are expressed as averages and standard deviations of four measurements of a representative batch. No statistical difference was observed across the concentration levels and NP types (two-way ANOVA). (c, d) Dopaminergic activity of pD-coated NPs. Dose−response curve of dopamine- or pD-coated NPs for activation of the (c) DRD1 and (d) DRD2 in HEK cells. Cyclic AMP accumulation data are expressed as percentage of the maximal response elicited by dopamine (b) or forskolin (c) as indicated.**

*in vivo* studies. The pD layer deposited on solid surfaces did not interfere with regular cell adhesion processes and survival of mouse osteoblasts, rat pheochromocytoma cells,[44] and human endothelial cells.[45] Moreover, pD coating prevented acute blood toxicity caused by quantum dots and inflammatory reactions to poly(lactic acid) films *in vivo*.[46] Consistent with these results, the NP-pD created at two levels of dopamine concentrations (0.25 and 0.5 mg/mL) had no significant effect on viability of NIH/3T3 fibroblasts in the NP concentration of 0.0001−0.1 mg/mL after 24 h (Figure 4a) or 72 h (Figure 4b) exposure. Even pD aggregates (*i.e.*, 100% pD) were not toxic in the concentration of 0.0001−0.1 mg/mL. This result indicates that pD coating did not have cytotoxic effects.

Dopamine is a well-known neurotransmitter. Although it was shown that dopamine monomer did not exist in the pD coating,[46] it was necessary to confirm that pD did not have any residual activity of dopamine. Therefore, bioassays measuring dopamine receptor activation were performed. These experiments were carried out in HEK293 (human embryonic kidney) cells expressing either the dopamine D1 receptor (DRD1) or the dopamine D2 receptor (DRD2). The DRD1 couples to stimulatory G proteins, which stimulate the production of cAMP through the activation of adenylyl cyclase. As shown in Figure 4c, HEK-D1 cells respond to dopamine by displaying a dose-dependent increase in the production of cAMP. In contrast, the pD-coated NPs were inactive and did not show any significant enhancement in the cAMP production by the DRD1 (Figure 4c). Similar functional assays were carried out using the DRD2, which couples to inhibitory G proteins to inhibit forskolin-stimulated cAMP production. Increasing concentrations of dopamine induced a dose-dependent decrease in cAMP accumulation. Consistent with the results from the DRD1 studies, the pD-coated NPs had no significant effects on DRD2-mediated inhibition of cAMP accumulation (Figure 4d).

A recent study demonstrates that the pD layer dissolves away in pH 5 or lower,[47] suggesting that the presence of a pD layer is unlikely to interfere with degradation of NPs or intracellular drug release. Moreover, it is reported that the median lethal dose ($LD_{50}$) of intravenously injected pD NPs was as high as 400−585 mg/kg, and they induced no signs of toxicity over one month after injection, indicating low acute and

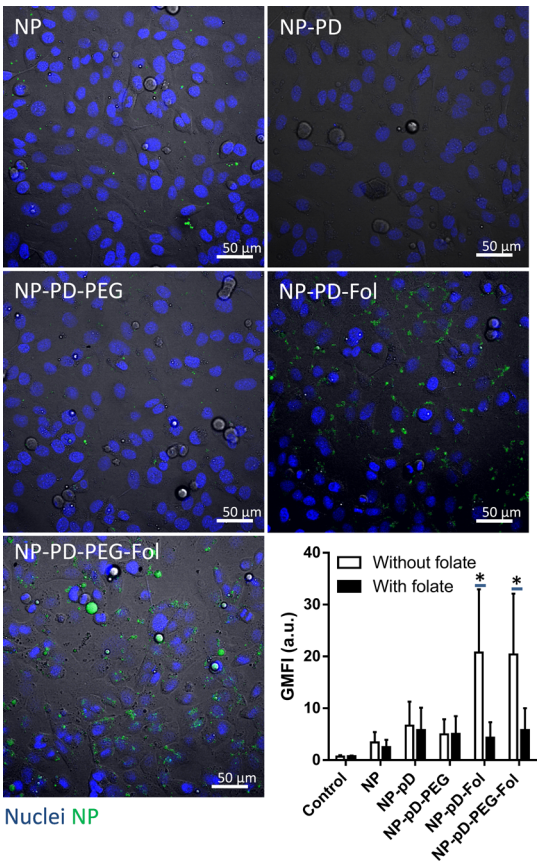


**Figure 5. Cellular uptake of fluorescently labeled NP, NP-pD, NP-pD-PEG, NP-pD-Fol, and NP-pD-PEG-Fol by KB cells, observed with confocal microscopy and flow cytometry. Flow cytometry data are expressed as averages and standard deviations of three batches of independently and identically prepared samples. *$p < 0.05$ by one-tailed paired *t* test.**

long-term toxicity *in vivo*.[48] While biodegradation and long-term toxicology of pD remain to be systematically investigated, our results and the literature consistently suggest that pD layers would present little biological hazard.

**Cellular Uptake of Functionalized Particles.** To evaluate whether the functionalized particles show the expected interactions with target cells, cellular uptake of the modified particles was observed using confocal microscopy and/or flow cytometry. Particles at concentrations used in this study had no influence on cell viability (Supporting Figure 6); therefore, the observed difference is attributable to the ability of viable cells to internalize the particles. We also note that the prime-coating with pD was performed in the same conditions (incubation in 0.5 mg/mL dopamine-Tris buffer (10 mM, pH 8.5) solution for 3 h at room temperature) for all particles to minimize any variation in pD thickness, which may affect the extent of cellular NP uptake otherwise.[49]

*NP, *NP-pD, and *NP-pD-PEG (* indicates fluorescein label) showed minimal cellular uptake by either KB cells (Figure 5) or HUVEC cells (Figure 6a). On the other hand, *NP-pD-Fol and *NP-pD-PEG-Fol showed a greater extent of cellular uptake by KB cells in both microscopy and flow cytometry (Figure 5), confirming the presence of functional folate on the NP surface. Co-treatment with folate (1 mM) selectively inhibited cellular uptake of *NP-pD-Fol and *NP-pD-PEG-Fol (Figure 5). This result indicates that the folate-modified NPs were taken up by KB cells *via* folate-receptor-mediated endocytosis. Similarly, *NP-pD-cRGD were taken up by HUVEC activated with TNF-α (hence expressing $\alpha_v\beta_3$ integrin[50]) to a greater extent than *NP or *NP-pD (Figure 6a). On the other hand, cRADyk, a control peptide with a similar molecular weight and isoelectric point to cRGDyk, did not contribute to cellular uptake of the modified NPs (*NP-pD-cRAD). This demonstrates that the increased cellular uptake of *NP-pD-cRGD was a result of specific cRGD interaction with $\alpha_v\beta_3$ integrin expressed on the activated HUVEC cells.

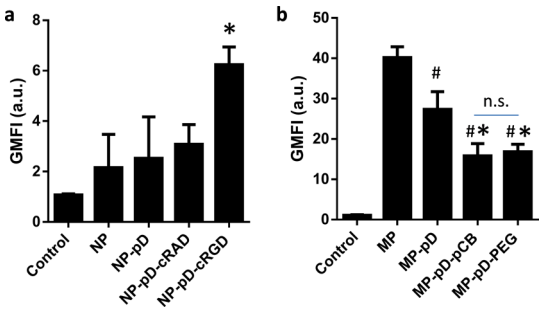


**Figure 6. (a) Cellular uptake of fluorescently labeled NP, NP-pD, NP-pD-cRAD, and NP-pD-cRGD by TNF-α-activated HUVECs. *$p < 0.005$ *vs* NP by two-tailed *t* test. (b) Cellular uptake of fluorescently labeled MP, MP-pD, MP-pD-pCB, and MP-pD-PEG by J774A.1 macrophages. #$p < 0.05$ *vs* MP; *$p < 0.05$ *vs* MP-pD; n.s.: not significant by two-tailed *t* test. Flow cytometry data are expressed as averages and standard deviations of three batches of independently and identically prepared samples.**

To evaluate the stealth effect of pCB, PLGA microparticles were modified with pCB and incubated with J774A.1 macrophages for measurement of their phagocytic uptake. Another set of MPs was modified with mPEG-$NH_2$ to compare with MP-pD-pCB. MPs with an average diameter of ~2 μm were used instead of NPs, since MPs are more readily taken up than NPs *via* phagocytosis;[51] thus, the effect of stealth polymers is best tested with MPs. As shown in Figure 6b, surface modification with pCB inhibited macrophage uptake of the particles effectively, and the extent of inhibition was similar to that of MP-pD-PEG. Interestingly, *MP-pD also showed reduced uptake by macrophages. Given the negative relationship between the extent of particle phagocytosis and the surface hydrophilicity,[52] the reduced *MP-pD uptake likely reflects the hydrophilic nature of the catechol and amine groups of the pD-coated surface.[18,53]

These results illustrate the versatility of the dopamine polymerization method in modifying the non-reactive surface of polymeric NPs. Using this method,

we recently reported a peritumorally activatable PLGA NP system, dual-functionalized with a cell-interactive peptide and an enzymatically removable PEG.[43] As demonstrated in this study, dual modification was carried out by simple incubation of core NPs in a mixture of two types of functional molecules with no need for new polymer synthesis or complex surface chemistry. The versatility of this surface modification method has an important implication for future NP development in that it can decouple NP formation and surface modification processes. In this way, polymers to make core NPs can be chosen according to the applications not constrained by the surface reactivity, and the surface modification may be performed on the preformed NPs, irrespective of their chemical identity.

## CONCLUSIONS

We used the dopamine polymerization method to functionalize the surface of PLGA NPs with folate, cRGD, and a stealth polymer. This method did not require modification of PLGA or chemical activation of the NP surface but involved only a brief incubation of NPs in alkaline solution of dopamine, followed by secondary incubation with the desired ligands. Thus formed NPs showed no cytotoxicity or residual bioactivity of dopamine and displayed expected interactions with target cells. Our study demonstrates that the dopamine polymerization method enables flexible surface modification of polymeric NPs with various functional ligands. With simplicity and versatility the dopamine polymerization method can expedite the development of NP drug carriers with functional surfaces.

## EXPERIMENTAL SECTION

**Materials.** PLGA (LA:GA = 65:35, carboxylic acid end group, molecular weight 118 kDa) was purchased from Lakeshore Biomaterials (Birmingham, AL, USA). (3-(4,5-Dimethylthiazol-2-yl)-2,5-diphenyltetrazolium bromide) (MTT), Hoechst 33342, and recombinant human tumor necrosis factor-alpha (TNF-α) were purchased from Invitrogen (Eugene, OR, USA). Polystyrene particles with an average diameter of 50 nm (PS50), 500 nm (PS500), and 1 μm (PS1000) were purchased from Polysciences (Warrington, PA, USA). Cyclo(Arg-Gly-Asp-D-Tyr-Lys) (cRGDyK) and cyclo(Arg-Ala-Asp-D-Tyr-Lys) (cRADyK) were purchased from Peptides International (Louisville, KY, USA). Folate-conjugated, amine-terminated polyethylene glycol (5 kDa, Fol-PEG-$NH_2$) and fluorescein-labeled poly(lactic-*co*-glycolic acid) (7 kDa, PLGA*) were purchased from Akina (West Lafayette, IN, USA). Methoxy-polyethylene glycol-amine (5 kDa, mPEG-$NH_2$) was purchased from JenKem Technology USA (Allen, TX, USA). Collagen I rat tail was purchased from BD Biosciences (San Jose, CA, USA). Poly(carboxybetaine methacrylate)-$NH_2$ (pCB, 9.4 kDa) was synthesized as described in the Supporting Information. Dopamine hydrochloride was purchased from Alfa Aesar (Ward Hill, MA, USA). All other materials were purchased from Sigma Aldrich unless specified otherwise.

**Preparation of Core PLGA Particles.** For preparation of ~200 nm NPs, 20 mg of PLGA was dissolved in 400 μL of dichloromethane (DCM). The polymer solution was added to 3 mL of a 5% PVA solution and immediately homogenized using a Sonics Vibracell probe sonicator (Sonics, Newtown, CT, USA) for 1 min, pulsing 4 s on and 2 s off at an amplitude of 80%. The emulsion was added to 5 mL of deionized water and stirred overnight to evaporate the remaining DCM. The NPs were then collected *via* centrifugation at 8161*g* for 30 min at 4 °C and washed twice in deionized water with centrifugation at 5223*g* for 20 min. For preparation of ~2 μm microparticles, the polymer solution was added to 5 mL of a 1% PVA solution and homogenized using a Silverson L4R laboratory mixer (East Longmeadow, MA, USA) for 1 min at 5000 rpm. The emulsion was dispersed in 10 mL of water and stirred overnight to evaporate the remaining DCM. The MPs were harvested *via* centrifugation at 1306*g* for 10 min at 4 °C and washed with deionized water twice. Fluorescently labeled particles for confocal microscopy and flow cytometry were prepared by replacing 8 mg of PLGA with the same amount of PLGA* (PLGA conjugated with fluorescein). All particles were stored as pellets at 4 °C and used in less than 24 h after preparation.

**Particle Surface Modification (Figure 1).** The core particles were prime-coated with pD by incubating 0.5 mg particles in 1 mL of dopamine hydrochloride solution in Tris buffer (10 mM, pH 8.5) for 3 h at room temperature with rotation. Dopamine concentration was fixed at 0.5 mg/mL unless specified otherwise. The pD-coated PLGA particles (NP-pD or MP-pD) were collected by centrifugation (NP-pD: 8161*g* for 20 min; MP-pD: 1306*g* for 10 min) at 4 °C. For surface functionalization, NP-pD or MP-pD were resuspended in Tris buffer (10 mM, pH 8.5), which contained different ligands (folate, mPEG-$NH_2$, Fol-PEG-$NH_2$, cRADyK, cRGDyK, or pCB). The final concentrations of particles and ligands were 1 and 2 mg/mL, respectively. After 30 min incubation at room temperature with rotation, particles were collected by centrifugation and washed with deionized water once. The functionalized NPs or MPs were designated as NP-pD-Fol, NP-pD-PEG, NP-pD-PEG-Fol, NP-pD-RAD, NP-pD-RGD, MP-pD-pCB, and MP-pD-PEG according to the ligand used for the functionalization.

**Quantification of Fluoresceinamine Incorporation.** A 0.5 mg amount of NP-pD was suspended in 1 mL of Tris buffer (10 mM, pH 8.5) containing fluoresceinamine in different concentrations (1−10 μg/mL) and incubated for 30 min at room temperature. The resulting NPs (NP-pD- FLA) were collected at 8161*g* for 20 min. Free (unincorporated) FLA was quantified by measuring the absorbance of each supernatant at 497 nm. The incorporated FLA into NP-pD- FLA was calculated by subtracting free FLA from the added FLA.

**Particle Characterization.** Particles were suspended in 1 mM phosphate buffer (pH 7.4), and their sizes and zeta potentials were measured by a Malvern Zetasizer Nano ZS90 (Worcestershire, UK). NP morphology was observed by scanning electron microscopy. NPs were sputter-coated with platinum for 60 s and visualized with a FEI Nova nanoSEM field emission scanning electron microscope (FEI Company, Hillsboro, OR, USA) using a high-resolution through-the-lens detector operating at a 5 kV accelerating voltage, ~3 mm working distance, and spot size 3. X-ray photoelectron spectroscopy was obtained with a Kratos Axis Ultra DLD spectrometer using monochromatic Al Kα radiation ($h\nu$ = 1486.58 eV). Survey and high-resolution spectra were collected at a fixed analyzer pass energy of 160 and 20 eV, respectively. A built-in Kratos charge neutralizer was used. Binding energy values were referenced to the Fermi edge, and charge correction was performed setting the C 1s peak at 284.80 eV. Data analysis was performed using the CasaXPS software (ver. 2.3.16).

**Cell Culture.** KB human epidermal carcinoma cells (ATCC, Manassas, VA, USA) were grown in Eagle's minimum essential medium complete medium supplemented with 10% fetal bovine serum (FBS). Human umbilical vein endothelial cells (HUVECs, ATCC) were grown in EGM-2 Bullet Kit complete medium. Culture plates were coated with 5 μg/cm$^2$ of rat tail collagen type I prior to cell culture. J774A.1 mouse macrophage cells and NIH/3T3 mouse fibroblast cells (ATCC) were grown in Dulbecco's modified Eagle medium (DMEM) complete medium supplemented with 10% FBS. These media were supplemented with 100 units/mL penicillin and 100 μg/mL streptomycin.

HEK293 (human embryonic kidney) cells stably expressing the dopamine D1 receptor (HEK-D1) or the long isoform of the dopamine D2 receptor (HEK-D2) were cultured in DMEM supplemented with 5% bovine calf serum (Thermo Fisher Scientific, Waltham, MA, USA), 5% fetal clone I (Thermo Fisher Scientific), and 1X antibiotic-antimycotic (Life Technologies, Green Island, NY, USA). In addition, the culture medium for the HEK-D1 cells contained 300 $\mu$g/mL G418 (Sigma, St. Louis, MO) and 2 $\mu$g/mL puromycin (Sigma), and the medium for the HEK-D2 cells contained 2 $\mu$g/mL puromycin. The cells were harvested using cell dissociation buffer (Life Technologies) and frozen in 1 mL aliquots of 10% DMSO (Sigma) in FBS (Thermo Fisher Scientific) until the day of the assay. All cells were subcultured at a ratio of 1:5 when they were 70−80% confluent.

**Cytotoxicity.** To examine the toxicity of the pD coating, the MTT assay was carried out with NIH/3T3 fibroblast cells incubated with the modified NPs. NIH/3T3 cells were plated in a 96-well plate at a density of 10 000 cells/well in 200 $\mu$L of complete medium. After overnight incubation, 10 $\mu$L of concentrated NP suspension was added to each well to provide NPs in a final concentration ranging from 0.0001 to 0.1 mg/mL. Cells were incubated with NPs for 24 h, washed twice with fresh medium, and incubated for an additional 48 h in NP-free complete medium. Another group of cells was incubated with NPs for 72 h. At the end of the incubation, the medium was replaced with 100 $\mu$L of fresh medium and 15 $\mu$L of 5 mg/mL MTT solution and incubated for 3.5 h. One hundred microliters of solubilization/stop solution comprising 20% SDS, 0.02% (v/v) acetic acid, and 50% (v/v) dimethyl sulfoxide (DMSO) was then added, and the plate was left in the dark overnight. The absorbance of solubilized formazan in each well was read with a SpectraMax M3 microplate reader (Molecular Devices, Sunnyvale, CA, USA) at a wavelength of 560 nm. The absorbance of the medium was subtracted from the absorbance of all wells. The measured sample absorbance was then normalized to the absorbance of control cells, which did not receive NPs.

**Dopaminergic Receptor Assay.** Pharmacological assays were carried out in HEK-D1 and HEK-D2 cells using the cAMP dynamic 2 kit from Cisbio Bioassays (Bedford, MA, USA). Briefly, cryopreserved cells were thawed and resuspended in Opti-MEM (Life Technologies). Cells were plated in 384-well plates (Perkin-Elmer, Waltham, MA, USA) at densities of 5000 and 4000 cells/well for HEK-D1 and HEK-D2 cells, respectively. The cells were incubated for 1 h at 37 °C in a humidified incubator with 5% $CO_2$. All assays were carried out in Opti-MEM containing 0.5 mM 3-isobutyl-1-methylxantine (Sigma) and 0.0025% (w/v) ascorbic acid (Sigma). The HEK-D1 assay measured cAMP in response to increasing concentrations of dopamine or the pD-coated NPs (PS50-pD, PS1000-pD, and NP-pD). For the HEK-D2 assays, 10 $\mu$M forskolin (Tocris Bioscience, Bristol, UK) was used to stimulate cAMP accumulation in the presence of dopamine or the NPs. The cells were incubated with dopamine or NPs for 1 h at room temperature, and cAMP accumulation was measured according to the manufacturer's instructions. Plates were read in a Synergy 4 (BioTek, Winoosky, VT, USA) at an excitation of 330 nm and emissions of 665 and 620 nm. A ratiometric analysis was carried out by dividing the 665 nm emission values by the corresponding 620 nm values. Unknown cAMP values were extrapolated from a cAMP standard curve. Assays were carried out in duplicate, and data analysis was done using GraphPad Prism 6 (GraphPad Software Inc., San Diego, CA, USA).

**Confocal Microscopy.** KB cells were seeded at a density of 80 000 cells/cm$^2$ in a 35 mm Petri dish. After overnight incubation, the medium was replaced with serum-free medium containing 0.4 mg/mL of fluorescently labeled NPs (*NPs). After 3 h incubation with NPs, the cells were then washed with media two times to remove free or loosely bound NPs. Hoechst 33342 was added to 2 $\mu$g/mL and incubated for 30 min prior to imaging. Confocal microscopy was performed using a Nikon A1R confocal microscope equipped with a Spectra Physics 163C argon ion laser and a Coherent CUBE diode laser. The *NPs were excited with a 488 nm laser, and the emission was read from 500 to 600 nm. Cell nuclei were excited with a 633 nm laser, and the emission was read from 650 to 750 nm.

**Flow Cytometry.** Cellular uptake of the functionalized NPs was quantitatively measured by flow cytometry. KB cells were plated in 24-well plates at a density of 50 000 cells/well, grown overnight, and incubated with *NP, *NP-pD, *NP-pD-PEG, *NP-pD-Fol, and *NP-pD-PEG-Fol suspended in serum-free medium. For competitive inhibition of NP uptake, folate was added to a final concentration of 1 mM simultaneously with NPs. HUVEC cells were plated in 24-well plates at a density of 50 000 cells/well and grown overnight. HUVEC cells were activated with TNF-$\alpha$ (4 ng/mL) for 4 h to induce $\alpha_v\beta_3$ integrin expression.[50] Cells were then incubated with *NP, *NP-pD, *NP-pD-cRGD, and *NP-pD-cRAD suspended in serum-free medium. J774A.1 cells were plated in 24-well plates at a density of 50 000 cells/well, grown overnight, and incubated with *MP, *MP-pD, *MP-pD-pCB, and *MP-pD-PEG suspended in serum-free medium. All particles were added at a concentration of 0.5 mg/mL. As a negative control, a group of cells was treated with fresh medium with no particles. After 3 h incubation, cells were trypsinized and analyzed with a flow cytometer (Beckman Coulter, FC 500, Indianapolis, IN, USA) with an FL-1 detector (Ex: 488 nm, Em: 525 nm). In all flow cytometry analyses, cell debris and free particles were excluded by setting a gate on the plot of side-scattered light *vs* forward scattered light. A total of 10 000 gated events were acquired for each analysis. The fluorescent amplifier of the FL-1 detector filter was adjusted to ensure that the negative cell population appeared in the first logarithmic decade. All experiments were performed in triplicate.

**Statistical Analysis.** All data were expressed as means ± standard deviations. Statistics were performed using ANOVA with a *t* test for means comparison unless specified otherwise. A value of $p < 0.05$ was considered statistically significant.

*Conflict of Interest:* The authors declare no competing financial interest.

*Acknowledgment.* This work was supported by NSF DMR-1056997, a grant from the Lilly Endowment, Inc. to College of Pharmacy, Purdue University, and Intramural Research Program (Global RNAi Carrier Initiative) of Korea Institute of Science and Technology. Part of this work was performed at the Purdue/CTSI Flow Cytometry and Cell Separation Facility, Life Science Microscopy Facility, and at the Surface Analysis Laboratory of the Birck Nanotechnology Center at Purdue University. The authors also thank generous support from the Purdue Center for Cancer Research and Dr. Dmitry Zemlyanov for financial and technical assistance with the XPS data acquisition and analysis.

*Supporting Information Available:* Supplementary methods and results are available free of charge *via* the Internet at http://pubs.acs.org.

## REFERENCES AND NOTES

1. Hong, R. L.; Huang, C. J.; Tseng, Y. L.; Pang, V. F.; Chen, S. T.; Liu, J. J.; Chang, F. H. Direct Comparison of Liposomal Doxorubicin with or without Polyethylene Glycol Coating in C-26 Tumor-Bearing Mice: Is Surface Coating with Polyethylene Glycol Beneficial? *Clin. Cancer Res.* **1999**, *5*, 3645–3652.
2. Hatakeyama, H.; Akita, H.; Harashima, H. A Multifunctional Envelope Type Nano Device (Mend) for Gene Delivery to Tumours Based on the Epr Effect: A Strategy for Overcoming the PEG Dilemma. *Adv. Drug Delivery Rev.* **2011**, *63*, 152–160.
3. Gu, F.; Zhang, L.; Teply, B. A.; Mann, N.; Wang, A.; Radovic-Moreno, A. F.; Langer, R.; Farokhzad, O. C. From the Cover: Precise Engineering of Targeted Nanoparticles by Using Self-Assembled Biointegrated Block Copolymers. *Proc. Natl. Acad. Sci. U.S.A.* **2008**, *105*, 2586–2591.
4. Sawant, R. M.; Hurley, J. P.; Salmaso, S.; Kale, A.; Tolcheva, E.; Levchenko, T. S.; Torchilin, V. P. "Smart" Drug Delivery Systems: Double-Targeted pH-Responsive Pharmaceutical Nanocarriers. *Bioconjugate Chem.* **2006**, *17*, 943–949.
5. Hatakeyama, H.; Akita, H.; Kogure, K.; Oishi, M.; Nagasaki, Y.; Kihira, Y.; Ueno, M.; Kobayashi, H.; Kikuchi, H.; Harashima, H. Development of a Novel Systemic Gene Delivery System

for Cancer Therapy with a Tumor-Specific Cleavable PEG-Lipid. *Gene Ther.* **2007**, *14*, 68–77.
6. Hatakeyama, H.; Akita, H.; Ito, E.; Hayashi, Y.; Oishi, M.; Nagasaki, Y.; Danev, R.; Nagayama, K.; Kaji, N.; Kikuchi, H.; *et al*. Systemic Delivery of siRNA to Tumors Using a Lipid Nanoparticle Containing a Tumor-Specific Cleavable PEG-Lipid. *Biomaterials* **2011**, *32*, 4306–4316.
7. Sahoo, S. K.; Labhasetwar, V. Enhanced Antiproliferative Activity of Transferrin-Conjugated Paclitaxel-Loaded Nanoparticles Is Mediated *via* Sustained Intracellular Drug Retention. *Mol. Pharmaceutics* **2005**, *2*, 373–383.
8. Rao, K. S.; Reddy, M. K.; Horning, J. L.; Labhasetwar, V. TAT-Conjugated Nanoparticles for the CNS Delivery of Anti-HIV Drugs. *Biomaterials* **2008**, *29*, 4429–4438.
9. Narayanan, S.; Binulal, N. S.; Mony, U.; Manzoor, K.; Nair, S.; Menon, D. Folate Targeted Polymeric 'Green' Nanotherapy for Cancer. *Nanotechnology* **2010**, *21*, 285107.
10. Cheng, J.; Teply, B. A.; Sherifi, I.; Sung, J.; Luther, G.; Gu, F. X.; Levy-Nissenbaum, E.; Radovic-Moreno, A. F.; Langer, R.; Farokhzad, O. C. Formulation of Functionalized PLGA-PEG Nanoparticles for *in Vivo* Targeted Drug Delivery. *Biomaterials* **2007**, *28*, 869–876.
11. Dhar, S.; Gu, F. X.; Langer, R.; Farokhzad, O. C.; Lippard, S. J. Targeted Delivery of Cisplatin to Prostate Cancer Cells by Aptamer Functionalized Pt(IV) Prodrug-PLGA-PEG Nanoparticles. *Proc. Natl. Acad. Sci. U.S.A.* **2008**, *105*, 17356–17361.
12. Mo, Y.; Lim, L. Y. Paclitaxel-Loaded PLGA Nanoparticles: Potentiation of Anticancer Activity by Surface Conjugation with Wheat Germ Agglutinin. *J. Controlled Release* **2005**, *108*, 244–262.
13. Hrkach, J.; Von Hoff, D.; Ali, M. M.; Andrianova, E.; Auer, J.; Campbell, T.; De Witt, D.; Figa, M.; Figueiredo, M.; Horhota, A.; *et al*. Preclinical Development and Clinical Translation of a PSMA-Targeted Docetaxel Nanoparticle with a Differentiated Pharmacological Profile. *Sci. Transl. Med.* **2012**, *4*, 128ra139.
14. Gullotti, E.; Yeo, Y. Beyond the Imaging: Limitations of Cellular Uptake Study in the Evaluation of Nanoparticles. *J. Controlled Release* **2012**, *164*, 170–176.
15. Farokhzad, O. C.; Cheng, J.; Teply, B. A.; Sherifi, I.; Jon, S.; Kantoff, P. W.; Richie, J. P.; Langer, R. Targeted Nanoparticle-Aptamer Bioconjugates for Cancer Chemotherapy *In Vivo*. *Proc. Natl. Acad. Sci. U.S.A.* **2006**, *103*, 6315–6320.
16. Zhang, Z.; Huey Lee, S.; Feng, S. S. Folate-Decorated Poly-(Lactide-co-Glycolide)-Vitamin E TPGS Nanoparticles for Targeted Drug Delivery. *Biomaterials* **2007**, *28*, 1889–1899.
17. Tosi, G.; Costantino, L.; Rivasi, F.; Ruozi, B.; Leo, E.; Vergoni, A. V.; Tacchi, R.; Bertolini, A.; Vandelli, M. A.; Forni, F. Targeting the Central Nervous System: *In Vivo* Experiments with Peptide-Derivatized Nanoparticles Loaded with Loperamide and Rhodamine-123. *J. Controlled Release* **2007**, *122*, 1–9.
18. Lee, H.; Dellatore, S. M.; Miller, W. M.; Messersmith, P. B. Mussel-Inspired Surface Chemistry for Multifunctional Coatings. *Science* **2007**, *318*, 426–430.
19. Lee, H.; Rho, J.; Messersmith, P. B. Facile Conjugation of Biomolecules onto Surfaces *via* Mussel Adhesive Protein Inspired Coatings. *Adv. Mater.* **2009**, *21*, 431–434.
20. Lu, L.; Li, Q. L.; Maitz, M. F.; Chen, J. L.; Huang, N. Immobilization of the Direct Thrombin Inhibitor-Bivalirudin on 316l Stainless Steel *via* Polydopamine and the Resulting Effects on Hemocompatibility *in Vitro*. *J. Biomed. Mater. Res. A* **2012**, *100*, 2421–2430.
21. Kang, K.; Choi, I. S.; Nam, Y. Biofunctionalization Scheme for Neural Interfaces Using Polydopamine Polymer. *Biomaterials* **2011**, *32*, 6374–6380.
22. Jiang, J.-H.; Zhu, L.-P.; Li, X.-L.; Xu, Y.-Y.; Zhu, B.-K. Surface Modification of PE Porous Membranes Based on the Strong Adhesion of Polydopamine and Covalent Immobilization of Heparin. *J. Membr. Sci.* **2010**, *364*, 194–202.
23. Zhu, L.-P.; Jiang, J.-H.; Zhu, B.-K.; Xu, Y.-Y. Immobilization of Bovine Serum Albumin onto Porous Polyethylene Membranes Using Strongly Attached Polydopamine as a Spacer. *Colloids Surf. B Biointerfaces* **2011**, *86*, 111–118.
24. Ren, Y.; Rivera, J.; He, L.; Kulkarni, H.; Lee, D.-K.; Messersmith, P. Facile, High Efficiency Immobilization of Lipase Enzyme on Magnetic Iron Oxide Nanoparticles *via* a Biomimetic Coating. *BMC Biotechnol.* **2011**, *11*, 63.
25. Yang, S. H.; Kang, S. M.; Lee, K.-B.; Chung, T. D.; Lee, H.; Choi, I. S. Mussel-Inspired Encapsulation and Functionalization of Individual Yeast Cells. *J. Am. Chem. Soc.* *133*, 2795−2797.
26. Xu, P.; Gullotti, E.; Tong, L.; Highley, C. B.; Errabelli, D. R.; Hasan, T.; Cheng, J.-X.; Kohane, D. S.; Yeo, Y. Intracellular Drug Delivery by Poly(Lactic-co-Glycolic Acid) Nanoparticles, Revisited. *Mol. Pharmaceutics* **2009**, *6*, 190–201.
27. Amoozgar, Z.; Park, J.; Lin, Q.; Weidle, J. H.; Yeo, Y. Development of Quinic Acid-Conjugated Nanoparticles as a Drug Carrier to Solid Tumors. *Biomacromolecules* **2013**, *14*, 2389–2395.
28. Amoozgar, Z.; Park, J.; Lin, Q.; Yeo, Y. Low Molecular-Weight Chitosan as a Ph-Sensitive Stealth Coating for Tumor-Specific Drug Delivery. *Mol. Pharmaceutics* **2012**, *9*, 1262–1270.
29. Lee, H.; Scherer, N. F.; Messersmith, P. B. Single-Molecule Mechanics of Mussel Adhesion. *Proc. Natl. Acad. Sci. U.S.A.* **2006**, *103*, 12999–13003.
30. Jiang, J.-H.; Zhu, L.-P.; Zhu, L.-J.; Zhu, B.-K.; Xu, Y.-Y. Surface Characteristics of Self-Polymerized Dopamine Coating Deposited on Hydrophobic Polymer Films. *Langmuir* **2011**, *27*, 14180–14187.
31. Bernsmann, F.; Ponche, A.; Ringwald, C.; Hemmerlé, J.; Raya, J.; Bechinger, B.; Voegel, J.-C.; Schaaf, P.; Ball, V. Characterization of Dopamine−Melanin Growth on Silicon Oxide. *J. Phys. Chem. C* **2009**, *113*, 8234–8242.
32. Ryu, J.; Ku, S. H.; Lee, M.; Park, C. B. Bone-Like Peptide/Hydroxyapatite Nanocomposites Assembled with Multi-Level Hierarchical Structures. *Soft Matter* **2011**, *7*, 7201–7206.
33. Hilgenbrink, A. R.; Low, P. S. Folate Receptor-Mediated Drug Targeting: From Therapeutics to Diagnostics. *J. Pharm. Sci.* **2005**, *94*, 2135–2146.
34. Shuhendler, A. J.; Prasad, P.; Leung, M.; Rauth, A. M.; Dacosta, R. S.; Wu, X. Y. A Novel Solid Lipid Nanoparticle Formulation for Active Targeting to Tumor $\alpha_v\beta_3$ Integrin Receptors Reveals Cyclic RGD as a Double-Edged Sword. *Adv. Healthcare Mater.* **2012**, *1*, 600–608.
35. Zhang, L.; Xue, H.; Gao, C.; Carr, L.; Wang, J.; Chu, B.; Jiang, S. Imaging and Cell Targeting Characteristics of Magnetic Nanoparticles Modified by a Functionalizable Zwitterionic Polymer with Adhesive 3,4-Dihydroxyphenyl-L-Alanine Linkages. *Biomaterials* **2010**, *31*, 6582–6588.
36. Li, G.; Cheng, G.; Xue, H.; Chen, S.; Zhang, F.; Jiang, S. Ultra Low Fouling Zwitterionic Polymers with a Biomimetic Adhesive Group. *Biomaterials* **2008**, *29*, 4592–4597.
37. Gao, C.; Li, G.; Xue, H.; Yang, W.; Zhang, F.; Jiang, S. Functionalizable and Ultra-Low Fouling Zwitterionic Surfaces *via* Adhesive Mussel Mimetic Linkages. *Biomaterials* **2010**, *31*, 1486–1492.
38. Zhang, Z.; Chen, S.; Jiang, S. Dual-Functional Biomimetic Materials: Nonfouling Poly(Carboxybetaine) with Active Functional Groups for Protein Immobilization. *Biomacromolecules* **2006**, *7*, 3311–3315.
39. Burzio, L. A.; Waite, J. H. Cross-Linking in Adhesive Quinoproteins: Studies with Model Decapeptides. *Biochemistry* **2000**, *39*, 11147–11153.
40. Liu, Y.; Ai, K.; Lu, L. Polydopamine and Its Derivative Materials: Synthesis and Promising Applications in Energy, Environmental, and Biomedical Fields. *Chem. Rev.* **2014**, 10.1021/cr400407a.
41. Shao, Q.; He, Y.; White, A. D.; Jiang, S. Difference in Hydration between Carboxybetaine and Sulfobetaine. *J. Phys. Chem. B* **2010**, *114*, 16625–16631.
42. Chen, S.; Li, L.; Zhao, C.; Zheng, J. Surface Hydration: Principles and Applications toward Low-Fouling/Nonfouling Biomaterials. *Polymer* **2010**, *51*, 5283–5293.
43. Gullotti, E.; Park, J.; Yeo, Y. Polydopamine-Based Surface Modification for the Development of Peritumorally Activatable Nanoparticles. *Pharm. Res.* **2013**, *30*, 1956–1967.

44. Ku, S. H.; Ryu, J.; Hong, S. K.; Lee, H.; Park, C. B. General Functionalization Route for Cell Adhesion on Non-Wetting Surfaces. *Biomaterials* **2010**, *31*, 2535–2541.
45. Ku, S. H.; Park, C. B. Human Endothelial Cell Growth on Mussel-Inspired Nanofiber Scaffold for Vascular Tissue Engineering. *Biomaterials* **2010**, *31*, 9431–9437.
46. Hong, S.; Kim, K. Y.; Wook, H. J.; Park, S. Y.; Lee, K. D.; Lee, D. Y.; Lee, H. Attenuation of the *in Vivo* Toxicity of Biomaterials by Polydopamine Surface Modification. *Nanomedicine* **2011**, *6*, 793–801.
47. Zheng, Q.; Lin, T.; Wu, H.; Guo, L.; Ye, P.; Hao, Y.; Guo, Q.; Jiang, J.; Fu, F.; Chen, G. Mussel-Inspired Polydopamine Coated Mesoporous Silica Nanoparticles as pH-Sensitive Nanocarriers for Controlled Release. *Int. J. Pharm.* **2014**, *463*, 22–26.
48. Liu, Y.; Ai, K.; Liu, J.; Deng, M.; He, Y.; Lu, L. Dopamine-Melanin Colloidal Nanospheres: An Efficient Near-Infrared Photothermal Therapeutic Agent for *in Vivo* Cancer Therapy. *Adv. Mater.* **2013**, *25*, 1353–1359.
49. Liu, X.; Cao, J.; Li, H.; Li, J.; Jin, Q.; Ren, K.; Ji, J. Mussel-Inspired Polydopamine: A Biocompatible and Ultrastable Coating for Nanoparticles *in Vivo*. *ACS Nano* **2013**, *7*, 9384–9395.
50. Danhier, F.; Vroman, B.; Lecouturier, N.; Crokart, N.; Pourcelle, V.; Freichels, H.; Jerome, C.; Marchand-Brynaert, J.; Feron, O.; Preat, V. Targeting of Tumor Endothelium by RGD-Grafted PLGA-Nanoparticles Loaded with Paclitaxel. *J. Controlled Release* **2009**, *140*, 166–173.
51. Tabata, Y.; Ikada, Y. Effect of the Size and Surface Charge of Polymer Microspheres on Their Phagocytosis by Macrophage. *Biomaterials* **1988**, *9*, 356–362.
52. Müller, R.; Rühl, D.; Lück, M.; Paulke, B. R. Influence of Fluorescent Labelling of Polystyrene Particles on Phagocytic Uptake, Surface Hydrophobicity, and Plasma Protein Adsorption. *Pharm. Res.* **1997**, *14*, 18–24.
53. Liao, Y.; Wang, Y.; Feng, X.; Wang, W.; Xu, F.; Zhang, L. Antibacterial Surfaces through Dopamine Functionalization and Silver Nanoparticle Immobilization. *Mater. Chem. Phys.* **2010**, *121*, 534–540.